Degradation of rhodamine B with manganese dioxide nanorods

V. Sabna, Santosh G. Thampi and S. Chandrakaran

ABSTRACT

This is an investigation on oxidative degradation of rhodamine B (RhB) by manganese dioxide (MnO_2) nanorods synthesized by redox co-precipitation method. Field emission scanning electron microscopy of MnO_2 nanorods at an electron voltage of 10 kV revealed a rod-like morphology for the synthesized nanoparticles. Fourier transform infrared spectra exhibited characteristic peaks of MnO_2. Surface area of MnO_2 nanorods was 277 m^2/g. Effect of various parameters like initial concentration and pH of RhB solution, time of contact between MnO_2 nanorods and RhB, dosage of MnO_2, and stirring speed on decolouration of RhB was evaluated in batch experiments. Rapid decolouration in the initial period of the reaction was observed due to the adsorption of RhB molecules onto the surface of MnO_2 nanorods followed by oxidative degradation. Percentage decolouration decreased with increase in initial concentration and increased with increase in dosage, speed of stirring the mixture and with increase in pH up to pH 7. Near complete decolouration was achieved at a dose of 0.5 g/L of MnO_2 nanorods from 20 mg/L RhB solution within 3 min. Observations fitted best to the pseudo second order kinetic model. This study could pave the way for development of cost-effective, nontoxic nanostructures for treatment of wastewaters containing RhB.

Key words | decolouration, manganese dioxide nanorods, rhodamine B

V. Sabna (corresponding author)
Santosh G. Thampi
S. Chandrakaran
Department of Civil Engineering,
National Institute of Technology Calicut,
Kozhikode, Kerala 673601,
India
E-mail: *sabnashareef123@gmail.com*

INTRODUCTION

Our Earth has been under the threat of contamination ever since the industrial revolution and with advancement in technologies and materials, the threat has assumed alarming proportions. At the start of industrial development, the nature of contaminants being discharged was such that the problem remained within the assimilative capacity of nature. However, as the contaminants being discharged became more complex, things started moving out of the natural assimilative capacity of the ecosystem. One of the industries that release toxic pollutants into the environment is the textile industry; it ranks top in the list of heavily polluting industries. The effluents from these industries contain a large amount of dye which is unused in the dyeing process (Mohan *et al.* 2007). Water contamination with textile dyes has several adverse effects. It reduces penetration of light through water. Dyes may be persistent in nature, mutagenic, carcinogenic, micro-toxic and may cause severe damage such as dysfunction of the kidneys, reproductive system, liver, brain and the central nervous system (Kadirvelu 2003; Dinçer *et al.* 2007). Rhodamine B is a cationic dye, having commercial and industrial applications. It causes skin irritation, sarcoma, digestive tract irritation, neurotoxicity and reproductive toxicity. Therefore, it is essential to remove rhodamine B from the wastewater generated by industries that use

doi: 10.2166/wh.2018.102

rhodamine B before discharging it to any water body. Several methods are available for the removal of dyes from effluents, such as coagulation, chemical oxidation, photocatalysis, irradiation, electrochemical destruction, ozonation, microbial degradation, membrane separation and ion exchange (Mahir *et al.* 2014). However, these processes are limited by sludge generation, high usage of energy, generation of dissolved oxygen, longer retention time, release of aromatic compounds, formation of by-products, high operational costs and operational difficulties (Mahir *et al.* 2014). Nanomaterials have been found to have wide applications as catalysts (Pradhan *et al.* 2001; Grunes *et al.* 2003; Astruc *et al.* 2005) for the degradation of different types of pollutants in water and wastewater. Particles in the nanometer size range have very large surface area, thereby offering many binding sites to the reacting species. Manganese dioxide, a transitional metal oxide in different shapes such as nanosheets (Saha & Pal 2014), αMnO_2, βMnO_2 and γMnO_2 (Cui *et al.* 2015), in combination with activated carbon (Asfaram *et al.* 2015), multiwalled carbon nanotubes (Sabna *et al.* 2016), graphene oxide (Liu *et al.* 2010), etc. can be used for the treatment of wastewater containing different types of pollutants. Oxidative degradation process takes place at the surface of MnO_2 after adsorption of the pollutant molecules (Stone & Morgan 1984; Li *et al.* 2008). The decolouration of methylene blue (Zhu *et al.* 2010) and malachite green (Saha & Pal 2014), oxidation of N-oxides (Zhang & Huang 2005) and polybrominated diphenyl ethers (Ahn *et al.* 2006), and formation of heavy metals (viz., As(III) and Cr(III)) (Fendorf & Zasoski 1992; Feng *et al.* 2006; Apte *et al.* 2006) to their higher oxidation states have also been studied by different types of MnO_2 nanomaterials. Some nanostructured MnO_2 materials have also been applied for Fenton-like catalytic degradation of rhodamine B, congo red, ethylene blue and methylene blue (Sui *et al.* 2009; Cao *et al.* 2010).

In this study, MnO_2 nanorods synthesized by redox co-precipitation method have been used for the oxidative degradation of rhodamine B. The effect of operating parameters such as the time of contact between the MnO_2 nanorods and the dye molecules, initial concentration of the dye in the aqueous solutions, pH of the aqueous solutions containing the dyes, dosage of MnO_2 nanorods, and speed of stirring the mixture of the dye and the MnO_2 nanorods was evaluated. Kinetic analysis of the oxidative degradation of these dyes using MnO_2 nanorods was performed by first order, second order, pseudo first order and pseudo second order kinetic models, and the results are reported in this paper.

MATERIALS AND METHODS

Materials

Manganese sulphate monohydrate ($MnSO_4 \cdot H_2O$), potassium permanganate ($KMnO_4$) and hydrogen peroxide (H_2O_2) procured from Merck were used for the synthesis of manganese dioxide (MnO_2) nanorods. Potassium nitrate (KNO_3), hydrochloric acid (HCl) and sodium hydroxide (NaOH) used for the determination of pH_{PZC} were also purchased from Merck. The dye, rhodamine B ($C_{28}H_{31}ClN_2O_3$, $\lambda_{max} = 550$ nm), was purchased from Sisco Research Laboratories Pvt. Ltd. Distilled water was used for the synthesis of MnO_2 nanorods and to prepare rhodamine B solutions of different concentrations.

Synthesis of MnO_2 nanorods

Manganese dioxide (MnO_2) nanorods were prepared by scaling down the redox co-precipitation method described in the literature (Parida *et al.* 1981; Gohari *et al.* 2014) and drying under ambient temperature. $MnSO_4$ solution was prepared by dissolving 30 g of $MnSO_4 \cdot H_2O$ in 250 mL distilled water. To this, $KMnO_4$ solution of pH 12.5 prepared by dissolving 20 g of $KMnO_4$ in 250 mL distilled water was added drop by drop under vigorous stirring. The dark brown mixture, formed as the addition of $KMnO_4$ was completed, was kept undisturbed overnight under ambient conditions in open air. The brown precipitate thus obtained was washed thoroughly until a clear supernatant with neutral pH was obtained. The mass was separated through centrifugation and dried in ambient air instead of drying in an oven at a higher temperature as in Parida's method (Parida *et al.* 1981).

Characterization of MnO_2 nanorods

Field emission scanning electron microscope (FESEM-HITACHI SU 6600, Dublin) with variable pressure field emission was used for the analysis of surface features of the MnO_2 nanorods. The sample of synthesized MnO_2 was sputter coated with gold for 40 s for inducing electrical conductivity with a sputtering unit. An electron voltage of 10 kV was applied during FESEM imaging of MnO_2 nanorods and 5 kV for commercial MnO_2. It is an important parameter for a material which acts as a catalyst or adsorbent; it is also important if the process involved in the removal of dye molecules is a function of surface area. The pH_{PZC} of MnO_2 nanorods was determined following the literature (Oliveira *et al.* 2010). 0.005 g MnO_2 nanorods were taken into five 50 mL Erlenmeyer flasks, each containing 10 mL of 0.03 M KNO_3 solution used as an electrolyte. The pH of the mixture of 0.03 M KNO_3 solutions and MnO_2 nanorods was adjusted to a range varying from 2.5 to 11.5 using dilute aqueous HCl and NaOH solutions ($pH_{initial}$). All the flasks were then shaken in an orbital shaker for 24 h at 250 rpm and then kept undisturbed for 1 h, after which the final pH of all the solutions was measured. A graph was plotted between $pH_{initial}$ (on X axis) and pH_{final} (on Y axis) of the 0.03 M KNO_3 solutions and the mixture of MnO_2 nanorods in 0.03 M KNO_3 solution. pH_{PZC} of the material is the value of pH corresponding to the point of intersection of the curves of $pH_{initial}$ and pH_{final} of the 0.03 M KNO_3 solutions and initial ($pH_{initial}$) and final pH (pH_{final}) of the mixture of MnO_2 nanorods in 0.03 M KNO_3 solution. Brunauer–Emmett–Teller (BET) surface area (m^2/g), pore volume (cm^3/g) and pore size (nm) were determined using 3000MMD/BSMR/0101-BET (Tristar USA). Chemical bonds in the MnO_2 nanorods were identified from the Fourier transform infrared (FTIR) spectra of MnO_2 nanorods obtained from the FTIR spectrophotometer (FT/IR-4100 A, JASCO, Germany).

Batch oxidation experiments

All the oxidative degradation experiments in batch mode were performed with 10 mL (working volume) of rhodamine B solution. A range of initial concentration of rhodamine B from 20 to 85 mg/L was fixed for evaluating the influence of time of contact between the nanorods and dye molecules on percentage decolouration. The concentration of the dye in the solution was measured after specific time intervals until equilibrium was reached during the degradation process using UV/VIS spectrophotometer (Lambda 35, Perkin Elmer) at a wavelength of 550 nm. The effect of dosage of MnO_2 nanorods on the degradation of rhodamine B was studied at dosages ranging from 0.5 to 2.0 g/L. Further, the effect of pH of the rhodamine B solution was evaluated under different pH values ranging from 3 to 8. Percentage degradation of the dye as percentage decolouration (%R) and the amount of dye degraded per unit quantity of the nanorods q_e (mg/g) at equilibrium were obtained using Equations (1) and (2), respectively.

$$\%\, R = \frac{C_i - C_t}{C_i} \times 100 \tag{1}$$

$$q_e\,(\mathrm{mg/g}) = \frac{C_i - C_e}{m} v \tag{2}$$

where C_i (mg/L), C_t (mg/L) and C_e (mg/L) are the initial concentration of the dye, concentration of the dye at time t and the concentration at equilibrium, respectively, m (g) is the mass of MnO_2 nanorods and $v(L)$ is the volume of the rhodamine B solution. Oxidative degradation of textile wastewaters may be affected by the presence of low molecular weight organic acids such as oxalic acids, citric acid, maleic acid, etc. These constituents compete for adsorption sites on the surface of the nanorods. The effect of low molecular weight acids was evaluated with oxalic acid and citric acid at two concentrations, 250 mg/L and 500 mg/L. Reusability of MnO_2 nanorods was investigated to determine how long (in terms of cycles of use) these nanorods can be used without reduction in their performance with respect to degradation of rhodamine B. Each cycle consisted of a reaction with 10 mL of 5 mg/L rhodamine B solution with 0.5 g/L of the nanorods for 1 min. The same MnO_2 nanorods were used in all cycles, after washing at the end of each cycle. The amount of dye degraded by the MnO_2 nanorods was compared with that by commercial MnO_2.

The rate of oxidative degradation of rhodamine B with MnO_2 nanorods was analysed using various kinetic models such as first order, second order, pseudo first order and

pseudo second order kinetic models. The linear equations of these models, presented in Table 1, were used, and different parameters of these models were determined.

The terms C_0 and C_t in the equations are concentrations of CV at time, $t = 0$ and $t = t$, respectively. q_t (mg/g) and q_e (mg/g) are amount of the dye at time t and at equilibrium, respectively, and k_1 (min^{-1}) and k_2 (g/mg·min) are the rate constants in the respective kinetic model equations. Linear equations of each of the models were plotted and the parameters of the models were determined. Non-linear equations of the models were used for determining the quantity of dye degraded per unit quantity of the MnO_2 nanorods by each of the models.

RESULTS AND DISCUSSION

Surface area analysis

Nitrogen adsorption–desorption isotherms on MnO_2 nanorods and commercial MnO_2 are presented in Figure 1(a) and 1(b), respectively. Surface area of the MnO_2 nanorods and commercial MnO_2 analysed using a BET surface area analyser shows that the prepared MnO_2 nanorods had very much higher surface area than the commercial MnO_2. This is evident from the degradation activity of the MnO_2 nanorods also. Results of the surface area analysis are presented in Table 2.

Table 1 | Linear equations of kinetic models

Kinetic model	Linear model
First order	$\ln\frac{C_t}{C_0} = k_1 t$
Second order	$\frac{1}{C_t} = \frac{1}{C_0} + k_2 t$
Pseudo first order (PFOM)	$\ln(q_e - q_t) = \ln q_e - k_1 t$
Pseudo second order (PSOM)	$\frac{t}{q_t} = \frac{1}{k_2 q_e^2} + \frac{t}{q_e}$

SEM analysis

FESEM micrographs of the synthesized MnO_2 nanorods and commercial MnO_2 are presented in Figure 2(a) and 2(b), respectively. The morphology of synthesized MnO_2 was similar to rod-like structures with a thickness of 20 nm and length more than 750 nm. However, the commercial MnO_2 consisted of particles of different sizes and structure, as seen in Figure 2(b). Since synthesized MnO_2 was found to have structures with a high aspect ratio, it has a larger surface area when compared with commercial MnO_2.

Determination of pH_{PZC}

pH_{PZC} of the MnO_2 nanorods was determined from the graph plotted between the $pH_{initial}$ and pH_{final} of KNO_3 and a mixture of MnO_2 nanorods in KNO_3 and MnO_2 nanorods (Figure 3), where the pH_{PZC} is given by the point where the two curves intersect each other. The pH_{PZC} of MnO_2 is observed to be 3.9. Thus, it is expected that the surface will have a net positive charge below pH 3.9, and a net negative charge above pH 3.9.

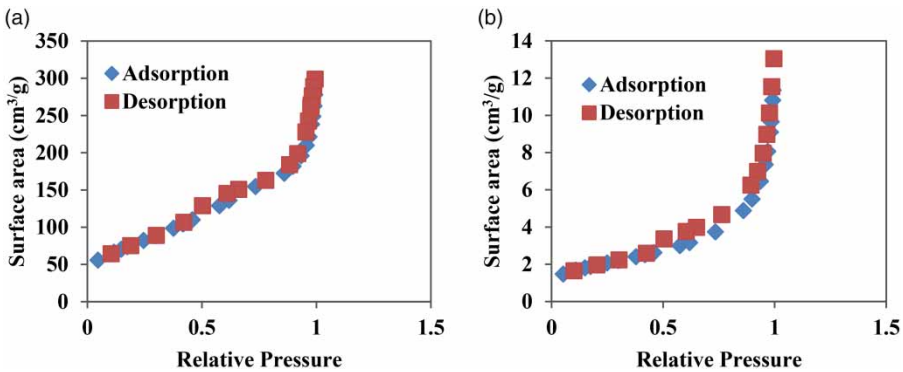

Figure 1 | Nitrogen adsorption–desorption isotherm: (a) MnO_2 nanorods and (b) commercial MnO_2.

Table 2 | BET surface area measurements of MnO_2 nanorods and commercial MnO_2

Material	Surface area (m^2/g)	Pore diameter (nm)	Pore volume (cm^3/g)
MnO_2 nanorods	277.87	5.379	0.374
Commercial MnO_2	6.96	8.145	0.015

FTIR analysis

FTIR spectroscopy is a technique used for the determination of characteristic bonds in molecules. FTIR spectral data were used to obtain information on bands present in MnO_2 nanorods. Important bands obtained in the FTIR spectra and the corresponding chemical bonds are presented in Figure 4.

Batch oxidative degradation experiments

Effect of contact time

Batch adsorption experiments were performed to evaluate the performance of MnO_2 nanorods in the oxidative degradation of rhodamine B from aqueous solutions. Percentage decolouration increased rapidly in the first 5 min of the reaction between the dye molecules and MnO_2 nanorods. However, percentage decolouration decreases with time as more and more of the nanorods are being utilized. Equilibrium was reached within approximately 20 min. Complete decolouration was observed with 20 mg/L rhodamine B solution of dosage 0.5 g/L within 3 min. At higher initial concentrations, a longer time of contact is required to attain equilibrium. Rapid increase in percentage decolouration in the initial period of the reaction was observed due to the adsorption of rhodamine B molecules onto the surface of the MnO_2 nanorods followed by oxidative degradation of these dye molecules on the surface of the MnO_2 nanorods. The time required for attaining maximum decolouration increased as the concentration of the dye in the solution was increased. The effect of time of contact between the MnO_2 nanorods and rhodamine B dye molecules on degradation of rhodamine B is presented in Figure 5(a).

Effect of initial concentration of rhodamine B solution

The initial concentration of rhodamine B solution affects the degradation of dye molecules by the MnO_2 nanorods and also the time required for attaining equilibrium. Percentage decolouration decreased from 100% for 20 mg/L dye solution to 60% for 85 mg/L dye solution for an adsorbent dosage of 0.5 g/L. For solutions with initial concentration 20 mg/L, the number of nanorods compared with the number of dye molecules was high, and not all the nanorods were utilized by the dye molecules, and so equilibrium was reached within 3 min. In all the other cases, the maximum number of dye molecules was degraded; however, the percentage of decolouration decreased with increase in the initial concentration of rhodamine B solution. The amount of rhodamine B degraded at equilibrium increased from 30 mg/g to 107 mg/g when the concentration of rhodamine B was increased from 20 to 75 mg/L for 0.5 g/L dosage of MnO_2 nanorods.

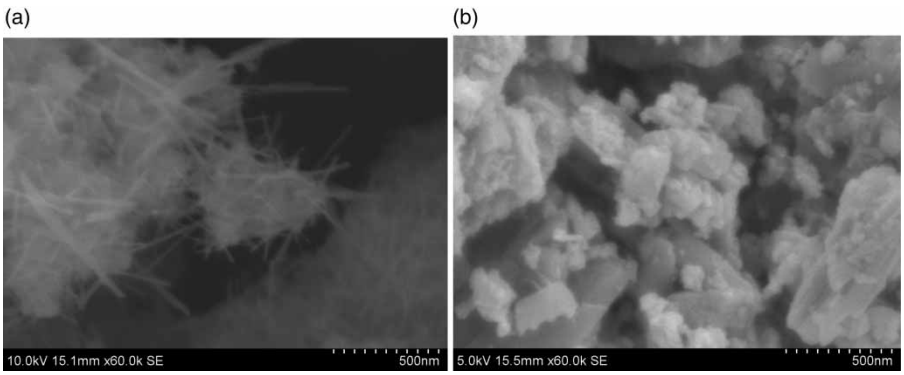

Figure 2 | FESEM images of (a) MnO_2 and (b) commercial MnO_2.

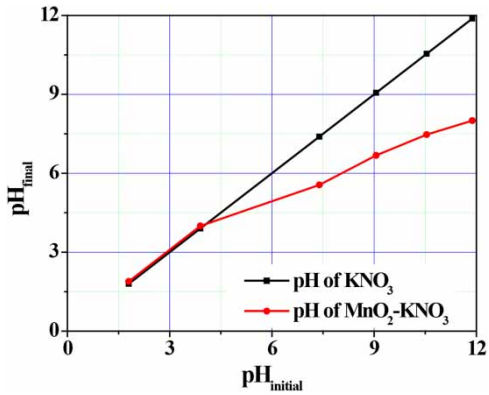

Figure 3 | Point of zero charge (pH_{PZC}) of MnO_2 nanorods.

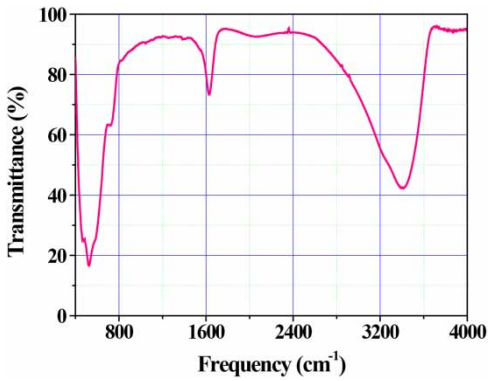

Figure 4 | FTIR spectra of MnO_2 nanorods.

This is because the ratio of nanorods to dye molecules in the 75 mg/L solution was low compared with that for 20 mg/L rhodamine B solution. Even after the initial concentration was increased to 85 mg/L, the amount of rhodamine B degraded at equilibrium remained the same (107 mg/g) because for initial concentration 75 mg/L and above, the nanorods are exhausted of the capacity to degrade the dye molecules. The results are presented in Figure 5(b).

Effect of pH of rhodamine B solution

The pH of the rhodamine B solution significantly affects degradation of the rhodamine B molecules by the MnO_2 nanorods. The H^+ ions present in a highly acidic rhodamine B solution can compete for the adsorption sites on the MnO_2 nanorods. The effect of pH of the rhodamine B solution on its decolouration was investigated to determine the range of pH in which the MnO_2nanorods can effectively degrade the dye and the change in percentage degradation of rhodamine B with pH. The study was conducted with rhodamine B solution of concentration 50 mg/L and dosage of MnO_2 nanorods 0.5 g/L. The results are presented in Figure 5(c).

Degradation of rhodamine B by MnO_2 nanorods was found to be significantly influenced by the pH of the rhodamine B solution. As the pH_{PZC} of MnO_2 nanorods was found to be 3.9, the MnO_2 nanorods have positive charge on their surface below this pH, causing repulsion between the particles and the cationic dye molecules. For this reason, the effect of pH was examined above the pH_{PZC} (i.e., >3.9) of the MnO_2 nanorods, when the surface of the MnO_2 nanorods would be negatively charged. Percentage decolouration increased with increase in pH from 4.7 to 7 due to a lower number of H^+ ions as the pH increases, and hence there is a possibility of increased electrostatic interaction between MnO_2 and the rhodamine B molecules, thereby making the process of adsorption and further degradation of rhodamine B more favourable. Percentage degradation decreased with increase in pH from 7 to 9.4 because at higher pH MnO_2 nanorods can interact with hydroxyl ions to form manganese hydrous oxides (oxo-metal chelation) (Subramanian *et al.* 2005). Percentage degradation of the dye increased from 92% to 97% with increase in pH up to 7. In the acidic pH range, excess H^+ ions compete with the cationic rhodamine B dye molecules for electrostatic attraction to the MnO_2 nanorods and so the percentage degradation of the dye decreases.

Effect of dosage of MnO_2 nanorods

The amount of nanorods added per unit volume of the dye solution is called dosage (g/L). It is an important factor in determining the cost of operation of treatment systems. Percentage degradation of rhodamine B increased with increase in the dosage of MnO_2 nanorods due to enhancement in the number of MnO_2 nanorods available for the oxidation of the dye molecules. The amount of rhodamine B dye degraded per unit weight of MnO_2 nanorods q_t, expressed in mg/g, decreased with increase in the dosage. This may be due to the

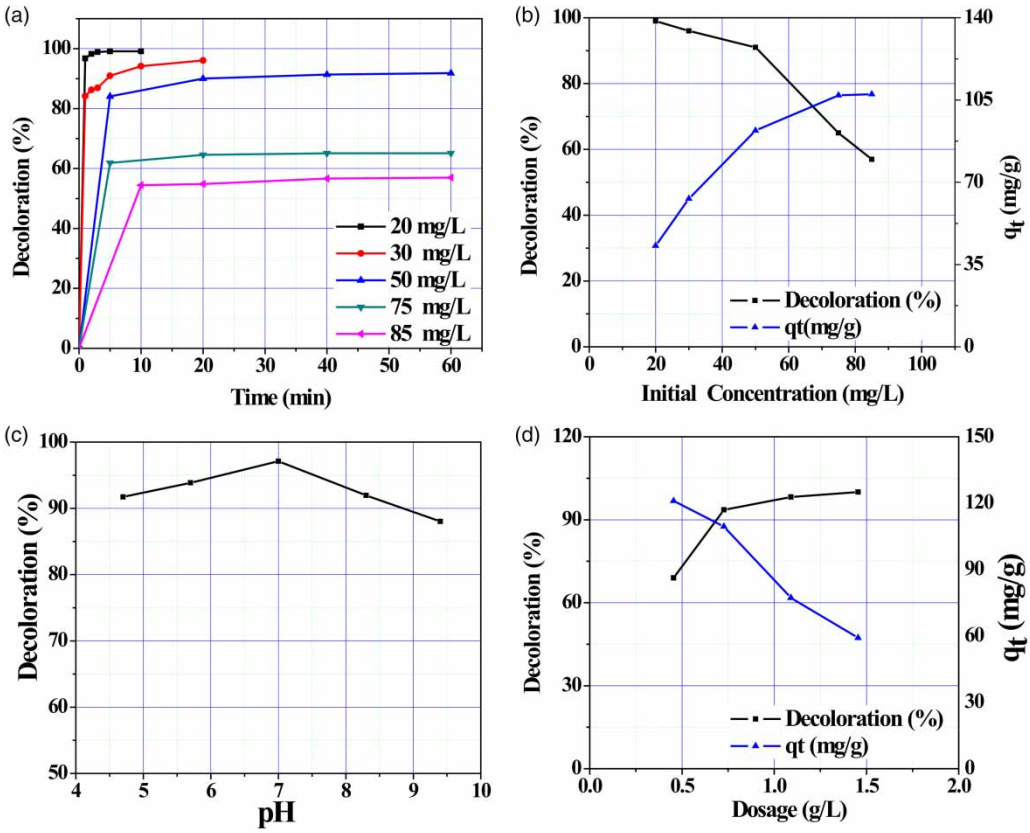

Figure 5 | Effect of (a) time of contact, (b) initial concentration, (c) pH and (d) dosage on percentage decolouration of rhodamine B.

aggregation of nanorods and decrease in the surface area for the adsorption of rhodamine B dye molecules on MnO_2 nanorods and for further degradation of the same. The results are presented in Figure 5(d).

Effect of low molecular weight acids in rhodamine B solution

Results of the investigation on the effect of oxalic acid and citric acid at two concentrations, 250 mg/L and 500 mg/L, on the percentage degradation are presented in Figure 6(a). It is observed that there was about a 30% decrease in the percentage degradation of the rhodamine B with oxalic acid in it from that observed in the case of the rhodamine B solution without oxalic acid. However, in the case of degradation of rhodamine B solution in the presence of citric acid in aqueous solutions, the percentage degradation of rhodamine B was almost equal to or higher than the percentage degradation of rhodamine B in the absence of it.

Reuse of MnO_2 nanorods

Reusability of any material for several cycles of treatment is important as far as the cost of treatment is concerned. The material should be reusable until it is exhausted of all its utility. Results of evaluation of the reusability of the MnO_2 nanorods in terms of percentage degradation of rhodamine B molecules after each cycle of oxidative degradation are presented in Figure 6(a). These results indicate that the material could be used up to six cycles without much reduction in the percentage degradation of rhodamine B molecules.

Comparison with commercial MnO_2

The percentage decolouration obtained by using MnO_2 nanorods was compared with that obtained for commercially available MnO_2. The results presented in Figure 6(c) indicate that MnO_2 nanorods exhibited higher efficiency in

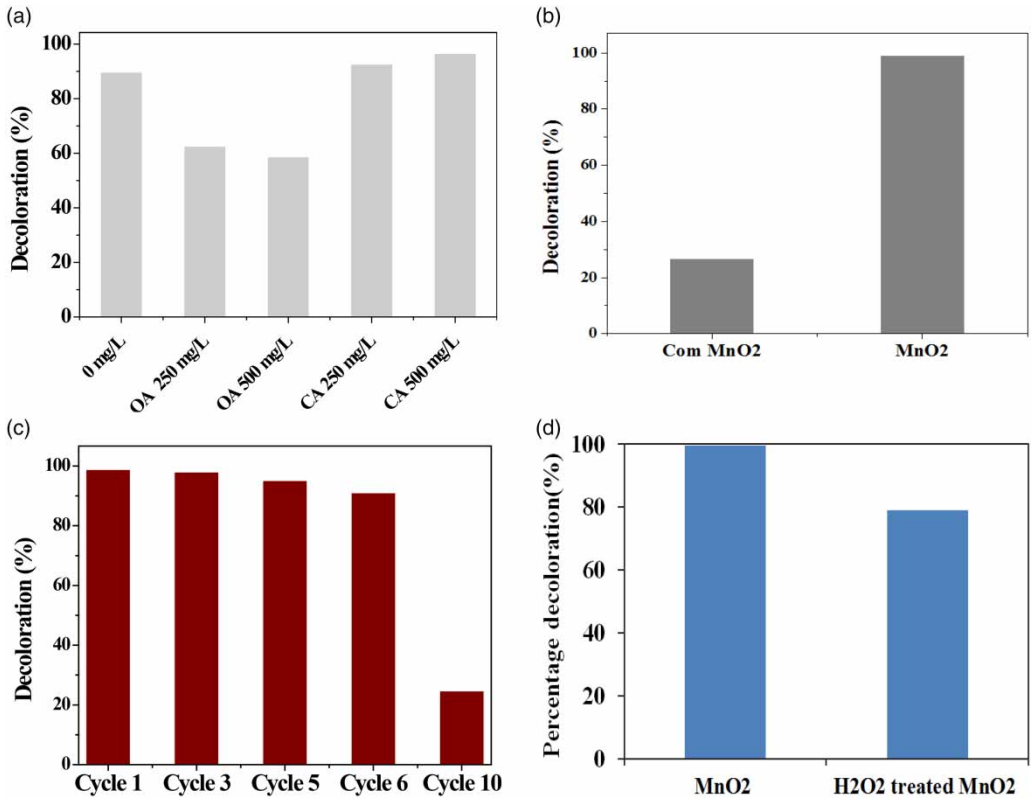

Figure 6 | (a) Effect of presence of acids on percentage decolouration, (b) reuse of MnO_2 nanorods, (c) comparison with commercial MnO_2 and (d) percentage decolouration of RhB with MnO_2 nanorods and MnO_2 nanorods treated with H_2O_2.

Table 3 | Coefficient of determination (R^2) of the kinetic models

Initial concentration (mg/L)	First order model	Second order model	Pseudo first order model	Pseudo second order model
20	0.324	0.940	0.906	1
30	0.620	0.846	0.737	0.999
50	0.525	0.744	0.850	0.999
75	0.000	0.000	0.839	1
85	0.000	0.000	0.503	0.999

terms of degradation of the dye (about 33% more removal) when compared with commercial MnO_2.

Mechanism of degradation

The reactivity of MnO_2 depends on the conditions during the preparation and the degree of hydration. The hydroxyl radicals present on the surface of MnO_2 nanorods are responsible for the degradation of dye molecules. Here, the

Table 4 | Parameters of kinetic models of oxidative degradation of rhodamine B

		Pseudo first order model			Pseudo second order models		
Initial concentration (mg/L)	q_e Exp (mg/g)	q_e cal, (mg/g)	k_1 (min^{-1})	R^2	q_e cal, (mg/g)	k_2 (g/mg·min)	R^2
20	43	19.95	1.93	0.906	43.6	1.75	1
30	63	19.27	0.31	0.737	66.0	0.08	0.999
50	92	32.96	0.12	0.850	99.4	0.03	0.999
75	107	47.09	0.22	0.839	110.0	0.08	1
85	107.5	47.31	0.03	0.503	110.5	0.02	0.999

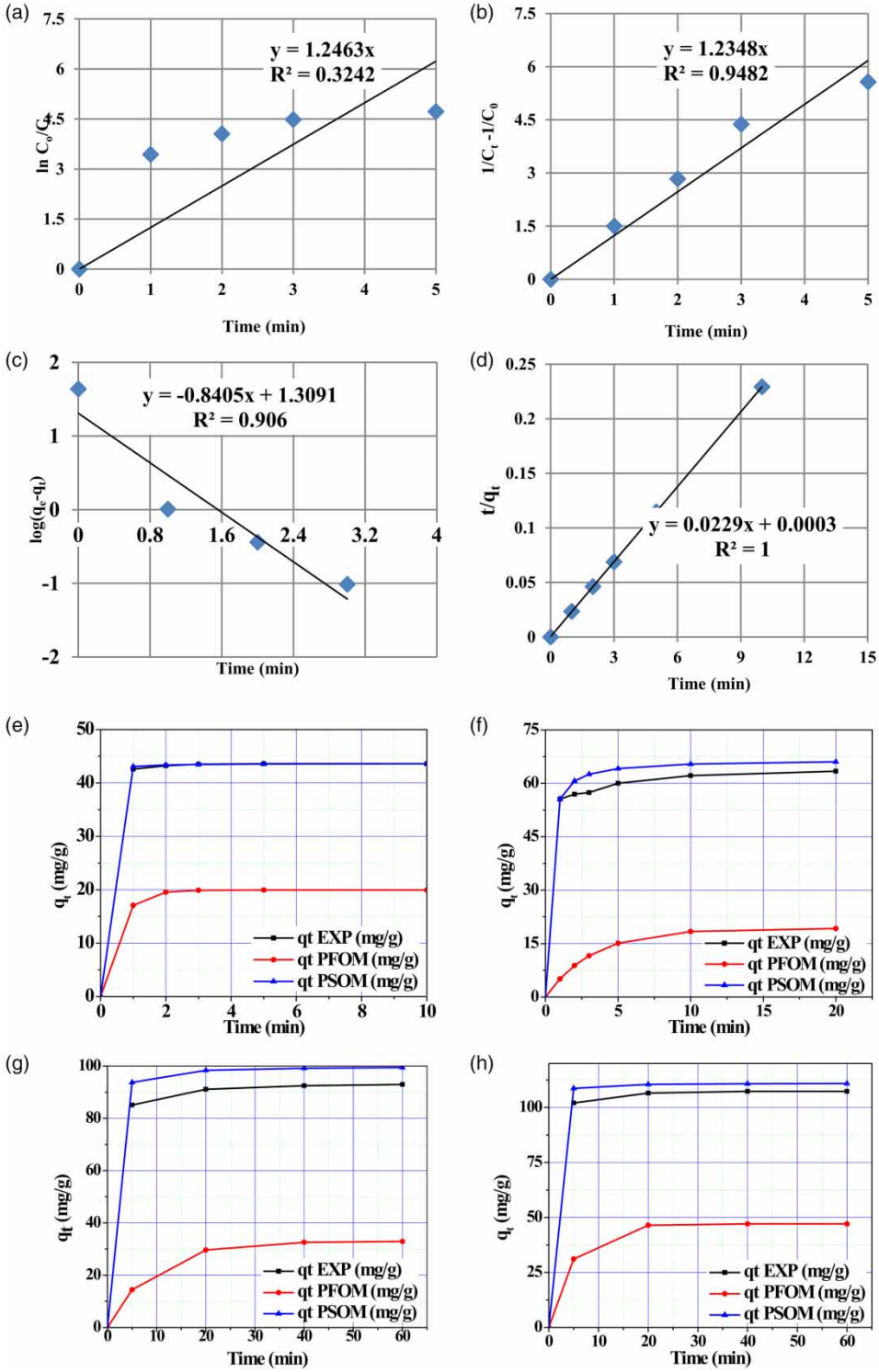

Figure 7 | Linear plot of (a) first order, (b) second order, (c) pseudo first order and (d) pseudo second order kinetic models. Comparison of q_t obtained from pseudo first order and pseudo second order kinetic models with the experimental data on the degradation of rhodamine B solution with initial concentration of (e) 20 mg/L, (f) 30 mg/L, (g) 50 mg/L and (h) 75 mg/L (dosage of MnO_2 nanorods = 0.5 g/L).

percentage decolouration of rhodamine B (concentration = 20 mg/L) during the oxidative degradation of MnO_2 nanorods treated with hydrogen peroxide decreased from 99 to 79. This may be due to the scavenging effect of hydrogen peroxide, which can scavenge the hydroxyl ions on the MnO_2 nanorods. The results are presented in Figure 6(d).

Kinetic analysis

Oxidative degradation processes of rhodamine B by MnO_2 nanorods were kinetically modelled using first order, second order, pseudo first order (PFOM) and pseudo second order (PSOM) kinetic models. Coefficients of determination of each of the kinetic models plotted with their linear model equations are presented in Table 3. The parameters of the pseudo first order and pseudo second order kinetic models, such as quantity of dye degraded per unit weight of the nanorods at equilibrium (q_e), rate constants, k_1 (pseudo first order kinetic model) and k_2 (pseudo first order kinetic model) and coefficient of determination (R^2) of the modelled values of q_e with pseudo first order and pseudo second order kinetic equations, are calculated from the linear plots and presented in Table 4. Parameters of the linear model equations are presented in Table 4.

The coefficient of determination for the pseudo second order model was relatively high and close to 1. The parameters of the first order, second order, pseudo first order and pseudo second order kinetic models, such as q_t (mg/g), q_e (mg/g), k_1 (min^{-1}) and k_2 (g/mg·min), were obtained by plotting the linear equations of these models (Figure 7(a)–7(d) for rhodamine B solution with initial concentration 50 mg/L). By using these parameters, the amount of dye degraded per unit weight of MnO_2 nanorods, q_t (mg/g), was estimated for each of the models.

CONCLUSION

Manganese dioxide (MnO_2) nanorods were prepared via the Parida method with a slight modification in the drying process. The rod-like shape of the synthesized MnO_2 could be observed from the FESEM micrographs. FTIR spectra indicated the formation of characteristic chemical bonds in the MnO_2 nanorods. pH_{PZC} of the material was found to be 3.9. Evaluation of the oxidative degradation characteristics of MnO_2 nanorods as a function of various process variables indicated that the percentage degradation of rhodamine B increased with increase in reaction time, dosage of MnO_2 nanorods and speed of stirring during the process. Percentage degradation increased with increase in the initial concentration of rhodamine B solution. pH of rhodamine B solution showed a positive effect on the percentage degradation of rhodamine B molecules up to pH 7, and it exhibited a decrease in the alkaline pH range. About 100% decolouration was achieved at 0.5 g/L dosage of MnO_2 nanorods from 20 mg/L rhodamine B solution in 3 min. Kinetic analysis of the oxidative degradation of rhodamine B with the MnO_2 nanorods indicated that the rate of reaction followed the pseudo second order kinetic model. Since the experimental data best suited the pseudo second order kinetic model and did not fit the first order kinetic model that well, it may be concluded that the degradation process started with the adsorption of rhodamine B (which usually follows the pseudo second order kinetic model) onto the surface of the MnO_2 nanorods and was followed by oxidative degradation at the surface of the nanorods.

ACKNOWLEDGEMENTS

The authors are grateful to the Department of Chemical Engineering, National Institute of Technology Calicut and Department of Chemistry, University of Calicut for their valuable support and assistance. The financial support to the first author by the University Grants Commission (UGC) (Grant Number F.2-11/2009 (SA-1)), Govt. of India, is also gratefully acknowledged.

REFERENCES

Ahn, M. Y., Filley, T. R., Jafvert, C. T., Nies, L., Hua, I. & Bezares-Cruz, J. 2006 Photodegradation of decabromodiphenyl ether adsorbed onto clay minerals, metal oxides, and sediment. *Environ. Sci. Technol.* **40**, 215–220.

Apte, A. D., Tare, V. & Bose, P. 2006 Extent of oxidation of Cr(III) to Cr(VI) under various conditions pertaining to natural environment. *J. Hazard. Mater.* **128**, 164–174.

Asfaram, A., Ghaedi, M., Hajati, S. & Goudarzi, A. 2015 Ternary dye adsorption onto MnO_2 nanoparticle-loaded activated carbon: derivative spectrophotometry and modeling. *RSC Adv.* **5** (88), 72300–72320.

Astruc, D., Lu, F. & Aranzaes, J. R. 2005 Nanoparticles as recyclable catalysts: the frontier between homogeneous and heterogeneous catalysis. *Angew. Chem. Int. Ed.* **44**, 7852–7872.

Cao, G., Su, L., Zhang, X. & Li, H. 2010 Hydrothermal synthesis and catalytic properties of a- and b MnO_2 nanorods. *Mater. Res. Bull.* **45**, 425–428.

Cui, H. J., Huang, H. Z., Fu, M. L. & Yuan, B. L. 2015 Decolorization of RhB dye by manganese oxides: effect of crystal type and solution pH. *Geochem. Trans.* **16** (1), 1–10.

Dinçer, A. R., Güneş, Y., Karakaya, N. & Güneş, E. 2007 Comparison of activated carbon and bottom ash for removal of reactive dye from aqueous solution. *Bioresour. Technol.* **98** (4), 834–839.

Fendorf, S. E. & Zasoski, R. J. 1992 Chromium (III) oxidation by β-MnO2 Part I: characterization. *Environ. Sci. Technol.* **26**, 79–85.

Feng, X. H., Zu, Y. Q., Tan, W. F. & Liu, F. 2006 Arsenite oxidation by three types of manganese oxides. *J. Environ. Sci.* **18**, 292–298.

Gohari, R. J., Halakoo, E., Lau, W. J., Kassim, M. A., Matsuura, T. & Ismail, A. F. 2014 Novel polyethersulfone (PES)/hydrous manganese dioxide (HMO) mixed matrix membranes with improved anti-fouling properties for oily wastewater treatment process. *RSC Adv.* **4** (34), 17587–17596.

Grunes, J., Zhu, J. & Somorjai, G. A. 2003 Catalysis and nanoscience. *Chem. Commun. (Camb).* **18**, 2257–2260.

Kadirvelu, K. 2003 Utilization of various agricultural wastes for activated carbon preparation and application for the removal of dyes and metal ions from aqueous solutions. *Bioresour. Technol.* **87**, 129–132.

Li, F., Liu, C., Liang, C., Li, X. & Zhang, L. 2008 The oxidative degradation of 2-mercaptobenzothiazole at the interface of β-MnO_2 and water. *J. Hazard. Mater.* **154** (1–3), 1098–1105.

Liu, C., Yu, Z., Neff, D., Zhamu, A. & Jang, B. Z. 2010 Graphene-based supercapacitor with an ultrahigh energy density. *Nano Lett.* **10** (12), 4863–4868.

Mahir, T., Dumaran, J. J., Devi, M. G., Rao, L. N., Pantelic, R. S., Meyer, J. C. & Kaiser, U. 2014 Dye removal from aqueous solution using low cost adsorbent. *J. Saudi Chem. Soc.* **18** (4), 1385–1391.

Mohan, N., Balasubramanian, N. & Basha, C. A. 2007 Electrochemical oxidation of textile wastewater and its reuse. *J. Hazard. Mater.* **147** (1–2), 644–651.

Oliveira, M., Machado, A. V. & Nogueira, R. 2010 Development of permeable reactive barrier for phosphorus removal. *Mater. Sci. Forum* **636–637**, 1365–1370.

Parida, B. R., Kanungo, K. M. & Sant, S. B. 1981 Studies on MnO_2-I chemical composition and other characteristics of some synthetic MnO_2 of various crystalline modifications. *Electrochim. Acta* **26**, 435–443.

Pradhan, N., Pal, A. & Pal, T. 2001 Catalytic reduction of aromatic nitro compounds by coinage metal nanoparticles. *Langmuir* **17** (5), 1800–1802.

Sabna, V., Thampi, S. G. & Chandrakaran, S. 2016 Adsorption of crystal violet onto functionalised multi-walled carbon nanotubes: equilibrium and kinetic studies. *Ecotoxicol. Environ. Saf.* **134**, 390–397.

Saha, S. & Pal, A. 2014 Microporous assembly of MnO_2 nanosheets for malachite green degradation. *Sep. Purif. Technol.* **134**, 26–36.

Stone, A. T. & Morgan, J. J. 1984 Reduction and dissolution of manganese(III) and manganese(IV) oxides by organics. 1. Reaction with hydroquinone. *Environ. Sci. Technol.* **18**, 450–456.

Subramanian, V., Zhu, H., Vajtai, R., Ajayan, P. M. & Wei, B. 2005 Hydrothermal synthesis and pseudocapacitance properties of MnO_2 nanostructures. *J. Phys. Chem. B* **109**, 20207–20214.

Sui, N., Duan, Y., Jiao, X. & Chen, D. 2009 MnO_2 prepared by hydrothermal method and electrochemical performance as anode for lithium-ion battery. *J. Phys. Chem.* **113**, 8560–8565.

Zhang, H. & Huang, C. H. 2005 Reactivity and transformation of antibacterial *N*-oxides in the presence of manganese oxide. *Environ. Sci. Technol.* **39**, 593–601.

Zhu, M.-X., Wang, Z., Xu, S.-H. & Li, T. 2010 Decolorization of methylene blue by δ-MnO_2-coated montmorillonite complexes: emphasizing redox reactivity of Mn-oxide coatings. *J. Hazard. Mater.* **181**, 57–64.

First received 30 December 2017; accepted in revised form 28 June 2018. Available online 9 August 2018